A Localized Zone of Increased Conductance Progresses over the Surface of the Sea Urchin Egg during Fertilization

DAVID H. MCCULLOH and EDWARD L. CHAMBERS

From the Department of Physiology and Biophysics, University of Miami School of Medicine, Miami, Florida 33101

ABSTRACT Although activation of a sea urchin egg by sperm leads to three phases of membrane conductance increase in the egg, the mechanism by which the sperm causes these conductance changes is not known. We used the loose patch clamp technique to localize the conductance changes in voltage clamped eggs. A patch of the egg's membrane was isolated from the bath by pressing the loose patch clamp pipette against the egg surface. Sperm added to the bath attached to the surface of the egg in a region other than at the isolated membrane patch. During phase 1 of the activation current, no changes of the membrane conductance were detected. At the time of, and subsequent to the onset of phase 2, large currents recorded between the interior of the patch pipette and the bath were attributed to changes of the seal resistance between the surface of the egg and the pipette. A local change of membrane conductance was observed during phase 2 despite the changes of seal resistance. During phase 2, the large amplitude and short duration of the local membrane conductance increase relative to the membrane conductance increase for the whole egg during phase 2 indicated that the conductance increase occurred over the entire surface of the egg, but not simultaneously. The time when the peak conductance for the membrane patch occurred, relative to the time of onset for phase 2 in the whole egg, depended on the distance, measured in a straight line, between the site of sperm attachment and the tip of the pipette. These data indicate that the localized conductance increase progressed over the surface of the egg from the site of sperm attachment to the opposite pole of the egg. It is proposed that the local conductance increase, the cortical reaction, and the change of seal resistance are all evoked by a common cytoplasmic message that progresses throughout the cytoplasm of the egg from the site of sperm attachment to the opposite pole of the egg.

Address reprint requests to Dr. David H. McCulloh, Department of Physiology and Biophysics, University of Miami School of Medicine, P.O. Box 016430, Miami, FL 33101.

J. GEN. PHYSIOL. © The Rockefeller University Press · 0022-1295/91/03/0579/26 $2.00
Volume 97 March 1991 579–604

INTRODUCTION

The activation potential that occurs within the first minute after insemination of the sea urchin egg (Steinhardt et al., 1971) consists of a depolarization in two phases (Chambers and de Armendi, 1979). During the initial phase (phase 1) which corresponds in duration to the latent period (Allen and Griffin, 1958), the attached sperm induces an increase of the egg's membrane conductance. During the following phase (phase 2), a major increase in membrane conductance occurs, accompanied by a wave of exocytosis that spreads around the egg from the site of sperm attachment (Lynn et al., 1988), causing elevation of the fertilization envelope. The initial depolarization is required for sperm entry to occur (Lynn and Chambers, 1984; Lynn et al., 1988), and a shift of potential to positive values prevents the entry of supernumerary sperm (Jaffe, 1976). The mechanism by which the sperm causes these changes in conductance is unknown.

The experiments described in this paper used the loose patch clamp technique to determine the localization of the membrane conductance changes associated with each of the two phases. Three different types of impedance were measured: (*a*) the conductance of the membrane for the whole egg, (*b*) the resistance or electrical tightness of the seal (R_s), which isolates a membrane patch at the surface of the egg from the bath, and (*c*) the conductance of this membrane patch (G_m). Our findings indicate that the initial membrane conductance increase (the phase 1 conductance increase measured for the whole egg) occurs locally at or near the site of sperm attachment. On the other hand, the major membrane conductance increase (phase 2 measured for the whole egg) occurs globally, over the entirety of the egg's surface, but *not* simultaneously, spreading from the site of sperm attachment to the opposite pole of the egg. This wavelike opening of channels advances around the egg shortly preceding the peak increase of seal resistance at the patch and near the time of the wave of cortical granule exocytosis. All three waves were found to traverse the egg at the same velocity. Our findings indicate that the message responsible for evoking the wavelike opening of channels, as well as the change of seal resistance, progresses throughout the cytoplasm of the egg.

These findings have been summarized previously in abstract form (McCulloh and Chambers, 1985, 1986*a*).

GLOSSARY

ANOVA	analysis of variance
arclen	distance between the site of sperm attachment and the location of patch pipette indentation, measured as the shortest arc over the surface of the egg between these two points
d	distance calculated using the Pythagorean theorem
d_a	distance between the site of sperm attachment and the location of patch pipette indentation, measured as the straight line chord through the cytoplasm of the egg
$d_{cytoplasm}$	distance between the site of sperm attachment and the membrane patch circumscribed by the loose patch clamp pipette, measured in a straight line through the cytoplasm of the egg
$d_{surface}$	distance between the site of sperm attachment and the membrane patch circumscribed by the loose patch clamp, measured over the surface of the egg

G conductance
G_m conductance of the membrane patch circumscribed by the patch clamp pipette
h distance in a horizontal dimension
I current
I_{pip} current flowing into or out of the loose patch clamp pipette
n number of values included in a determination
π the ratio of a circle's circumference to its diameter
piplen the distance between the location of patch pipette indentation at the surface of the egg and the membrane patch circumscribed by the orifice of the loose patch clamp pipette, measured along the pipette
R resistance
R_{pip} resistance of the loose patch clamp pipette
R_s resistance of the seal formed between the surface of the egg and the tip of the loose patch clamp pipette
v distance measured in a vertical dimension
V voltage
V_m membrane potential of the whole egg and the membrane patch
V_{pip} the amplitude of a command potential step applied to the patch pipette

METHODS

Physiological Solution

The seawater used in the experiments was collected from the Gulf Stream 3–5 miles offshore from Miami, FL. 10 mM Tris [hydroxymethyl] methylamino propane sulfonic acid (TAPS) was added to the seawater and pH was adjusted to 8.3.

Preparation of Gametes

Gametes were prepared essentially as described previously (McCulloh, 1989). Sea urchins (*Lytechinus variegatus*) were collected from the waters near Miami and maintained in seawater aquaria at 22°C. The coelomic cavity was exposed by removal of Aristotle's lantern with a pair of scissors. The coelomic cavities of females containing ripe ovaries were rinsed with 0.55 M KCl and then each female was inverted and suspended over a beaker filled with seawater. Eggs subsequently shed by each female were collected at the bottom of the beaker.

The testes of males were removed, blotted on filter paper to remove excess fluid, and maintained in Syracuse dishes at 4°C until aliquots of semen were diluted before insemination.

Only batches of eggs and sperm that resulted in 99–100% elevation of fertilization envelopes and normal cleavage in test inseminations were used.

The jelly coats of an aliquot of the eggs were partially removed by repeatedly inverting the egg suspension several times in a centrifuge tube (McCulloh, 1989). Several hundred dejellied eggs were pipetted into a plastic Petri dish (55 mm wide and 8 mm deep; Falcon Labware, Oxnard, CA) containing ~2 ml seawater. After mounting the dish on the stage of an inverted microscope, the eggs (maintained at 22°C) were observed using a long working-distance 40× planachromat objective and 10× oculars (Carl Zeiss, Inc., Thornwood, NY).

Electrophysiological Methods and Procedures

The bath (the Petri dish containing seawater and dejellied eggs) was mounted on the microscope stage (see above) and electrically connected to a virtual ground by means of two separate Ag/AgCl wire coils (one to sense the bath potential, the other to pass current, which

controlled the bath potential), both contained within a Pasteur pipette (tip diameter ~2 mm) containing seawater and "plugged" at its tip by 1% agar gelled in seawater.

Loose patch clamp. The loose patch clamp technique (Neher and Lux, 1969; Fishman, 1975; Stühmer et al., 1983; Whitaker and Steinhardt, 1983) was used to record the current from small regions of the plasma membrane. Loose patch clamp pipettes pulled by a two-stage protocol were heat polished to a tip diameter of 5–10 μm. The external surface of the tip of the pipette was coated with a 0.1% solution of polylysine (70,000–200,000 mol wt; Sigma Chemical Co., St. Louis, MO). Although the use of polylysine did not remarkably increase the resistance of the seal between the pipette and the surface of the egg, it did prolong the duration over which the seal resistance remained stable (> 1 h). Patch pipettes were filled with seawater.

After immersing the tip of the patch pipette in the bath, the resistance of the pipette (R_{pip}) was monitored by stepping the command voltage (5 mV) applied to the interior of the pipette. The amplitude of the voltage step (V_{pip}), divided by the amplitude of the resulting pipette current (I_{pip}), measured R_{pip}. The values for R_{pip} amounted to 0.35 ± 0.015 MΩ (n = 75). The tip of a patch pipette (after its resistance had been measured) was pushed against the surface of an egg, which adhered to the bottom of the dish. Suction was applied (approximately −2 cm of H_2O) to the interior of the pipette. The suction was controlled by a "U" tube manometer filled with water. The "U" tube was connected with the interior of a pipette holder equipped with a side arm (E.W. Wright, Bridgeport, CT) by means of polyethylene tubing containing an intervening air gap. To attain an adequate seal the pipette was advanced to deeply indent the surface of the egg (Fig. 1). The resistance of the seal between the pipette and the egg surface (R_s) was then determined by stepping V_{pip} and measuring the amplitude of the resulting I_{pip} as described below. Overall, seal resistances averaged 4.5 ± 0.38 MΩ (n = 75), on the average 15 ± 1.7 times R_{pip}. In experiments where the conductance of the membrane patch was to be measured, R_s's that were considered adequate amounted to 3.4 ± 0.58 MΩ (n = 14), or 12 ± 1.7 times the resistance of the pipette. (If only the seal resistance was to be measured, seals 5–10 times the pipette resistance could also be used.)

Removal of the vitelline coats from the unfertilized eggs by using 10 mM dithiothreitol, pH 9.2 (Epel et al., 1970), or 0.01% pronase, did not significantly improve the seals. Moreover, these treatments often decreased the input resistance of the unfertilized eggs. Therefore, these treatments were not used.

The potential of the patch clamp pipette (when not applying voltage steps) was voltage clamped at a potential as close to the bath potential (nominal 0 mV) as possible. This was done by adjusting the command potential for the pipette to a value at which I_{pip} equaled the current level recorded using the patch clamp with the tip of the patch pipette suspended in the air. However, slight potential differences (< 1 mV) between the pipette interior and the bath could not be eliminated when the pipette was in the bath or pushed against the egg, because of the low impedance (R_s) between the virtual ground devices in the patch clamp headstage and the bath.

Voltage clamp of the entire plasma membrane of the egg. If the seal resistance was adequate (see above) after the patch clamp pipette was in place, an intracellular glass electrode containing 0.5 M K_2SO_4, 20 mM NaCl, and 0.5 mM K citrate with a resistance of 20–30 MΩ was inserted into the cytoplasm of the egg as described previously (Lynn and Chambers, 1984; McCulloh et al., 1987; Lynn et al., 1988; McCulloh, 1989), and the membrane potential of the whole egg (including that of the patch) was voltage clamped at 0 or −20 mV by means of the single electrode switched voltage clamp technique (DAGAN Corp., Minneapolis, MN; Wilson and Goldner, 1975). The potential across the entire plasma membrane of the egg was voltage clamped to measure the sum of all currents through the membrane and not through the loose patch clamp pipette's seal resistance (measured in series with the microelectrode but not in the bath), as well as to measure the membrane resistance before and during insemination, as

described by Lynn and Chambers (1984), McCulloh et al. (1987), Lynn et al. (1988), and McCulloh (1989).

The membrane conductance of the whole egg was measured by stepping the command voltage between 0 and −20 mV and determining the amplitude of the resulting current, which

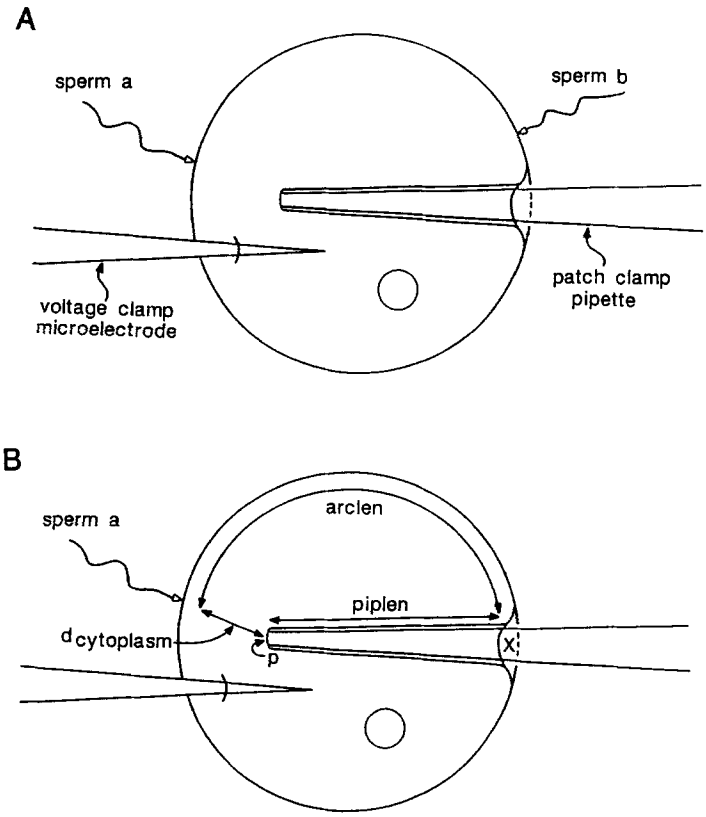

FIGURE 1. Configuration for patch clamp recording. (*A*) Sperm added to the bath can attach to the egg's surface at any position other than at the membrane circumscribed by the orifice of the pipette. Two possible positions are labeled (*sperm a, sperm b*). The tip of the loose patch clamp pipette is pushed against the surface of the egg, indenting its surface and causing a deep invagination in the surface of the egg from the location of indentation. After positioning of the loose patch clamp pipette, a microelectrode was inserted into the cytoplasm of the egg. (*B*) The distance in a straight line through the cytoplasm ($d_{cytoplasm}$) between the site of attachment for sperm *a* and the membrane patch (*p*) at the tip of the pipette was determined using Eq. 8. The distance between sperm *a* and *p* was also determined following the surface of the egg using Eq. 10 and arclen (the length of the shortest arc over the surface of the egg between sperm *a* and the location of pipette indentation at *X*) and piplen (the distance between *X* and *p*).

traversed the membrane of the whole egg. Simultaneously, the membrane conductance of the patch (G_m) was measured, with the external surface of the patch voltage clamped at nominal 0 mV, from the amplitude of the current pluses that flowed in the patch pipette in response to the voltage step (V_m) applied to the whole egg (see below).

Determination of the seal resistance. The equivalent circuit for the recording configuration used to measure the seal resistance (R_s) from the amplitude of the current pulse (I_{pip}) that occurs in response to a command voltage step (V_{pip}) applied to the pipette is shown in Fig. 2 *A* (abbreviations given in legend), where:

$$I_{pip} = \frac{V_{pip}(R_s + 1/G_m)}{R_{pip}R_s + R_{pip}/G_m + R_s/G_m} \quad (1)$$

Since $1/G_m$ for the patch of membrane ($1/G_m$ = resistance of the membrane patch) is several orders of magnitude larger than R_s and R_{pip}, the values of the numerator and the denominator are essentially determined only by the terms containing $1/G_m$:

$$I_{pip} = \frac{V_{pip}/G_m}{R_{pip}/G_m + R_s/G_m} \quad (2)$$

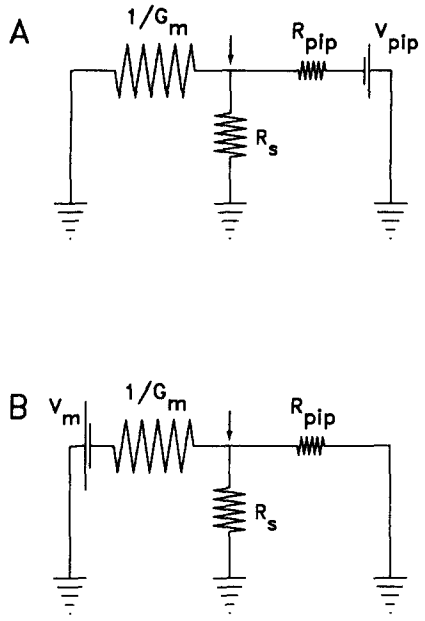

FIGURE 2. Equivalent circuits with patch pipette pressed against the surface of the egg (as shown in Fig. 1). Sizes of the resistor symbols indicate which resistances are largest, intermediate, and smallest. Arrow indicates the site of seal between the pipette tip and the egg's membrane. (*A*) For measurement of seal resistance (R_s) by stepping the potential inside the patch pipette (V_{pip}). (*B*) For measurement of the conductance of the membrane patch (G_m) by stepping the clamped membrane potential (V_m) of the whole egg.

Since $1/G_m$ cancels from both the numerator and the denominator:

$$I_{pip} = \frac{V_{pip}}{R_{pip} + R_s} \quad (3)$$

Therefore,

$$R_s = \frac{V_{pip}}{I_{pip}} - R_{pip} \quad (4)$$

In brief, because of the very high resistance ($1/G_m$) of the membrane patch, the seal resistance can be considered to be in series with the pipette resistance. Consequently, subtraction of the pipette resistance (assumed to remain constant) from the total resistance (with the pipette

pressed against the egg surface) gives the seal resistance when current is passed between the patch pipette and the bath by stepping the pipette potential by ~1 mV.

Determination of the conductance of the membrane patch. Because of the low seal resistance relative to the very high resistance ($1/G_m$) of the patch of egg membrane, it clearly was not reasonable to attempt to compute the flow of current through the membrane patch from the pipette current in response to voltage steps applied to the interior of the patch clamp pipette. However, by stepping the membrane potential of the voltage clamped whole egg, and maintaining the interior of the patch clamp pipette at nominal 0 mV, the current that passes through the membrane patch preferentially flows through the pipette (I_{pip}) rather than through the seal of higher resistance (10–15-fold greater). With this recording configuration (Fig. 2 *B*):

$$I_{pip} = \frac{\Delta V_m}{\dfrac{1}{G_m} + \dfrac{R_{pip}R_s}{R_{pip} + R_s}} \times \frac{R_s}{R_{pip} + R_s}$$

$$= \frac{\Delta V_m R_s}{\dfrac{R_{pip}}{G_m} + \dfrac{R_s}{G_m} + R_{pip}R_s} \tag{5}$$

Since $1/G_m$ is several orders of magnitude larger than R_{pip} and R_s, the value of the denominator is essentially determined by the terms containing $1/G_m$. Hence, the equation simplifies to:

$$I_{pip} = \Delta V_m G_m \frac{R_s}{R_{pip} + R_s} \tag{6}$$

and

$$G_m = \frac{I_{pip}}{\Delta V_m} \times \frac{R_{pip} + R_s}{R_s} \tag{7}$$

Since the resistance of the seal between the unfertilized egg and the pipette tip was 10–15 times that of the pipette resistance, the ratio $(R_{pip} + R_s)/R_s$ amounted to 1.06 to 1.1. Consequently, as long as the seal resistance did not significantly decrease, measurement of the ratio $I_{pip}/\Delta V_m$ alone underestimates G_m by only 6–10% (essentially within experimental error).

Determination of the surface area of the membrane patch. The surface area of the membrane patch as a fraction of the surface area of the whole unfertilized egg was estimated by dividing the conductance of the patch by that of the whole egg (both determined using slow voltage ramps of 110 mV applied to the whole egg membrane potential). For a patch pipette 5–10 μm in diameter at the tip, the surface area of the patch estimated by this method was 0.55 ± 0.09% (n = 7) of the surface area of the whole egg. For comparison, the surface area of a smooth circular surface 10 μm in diameter is 0.38% of the surface area of a smooth sphere 114 μm in diameter. Therefore, the region of recording may extend beyond the rim of the pipette.

Insemination of the Egg during Electrical Recording

The egg was inseminated while recording from the whole egg voltage clamp as well as the patch clamp, with voltage command steps applied either to the whole cell or the patch clamp pipette, or both. Sperm were prepared by diluting 10 μl dry sperm in 40 ml of seawater, and then a 10-μl aliquot of the dilution was pipetted into the bath within 5 mm of the egg. At 30 s to 1 min after the onset of the whole egg current, a fertilization cone started to elevate at the site of the

attached sperm, which caused the electrophysiological response. If more than one sperm caused an electrophysiological response, the results from that egg were not used.

Measurement of the Distance between the Site of Attachment of the Fertilizing Sperm and the Tip of the Patch Pipette

2–3 min after the onset of the whole egg current, after the electrical recordings had been completed, the position of the fertilizing sperm (indicated by the presence of a fertilization cone) and the tip of the patch pipette were measured using an ocular micrometer. The vertical distance was determined by noting the required number of turns of the microscope's calibrated fine focus knob to change the focal plane from that of the base of the fertilization cone to that of the tip of the patch pipette. The shortest distance between the sperm and the tip of the patch pipette was determined either (*a*) linearly through the cytoplasm, or (*b*) over the surface of the egg, as follows:

(*a*) The distance ($d_{\text{cytoplasm}}$) between the sperm and the tip of the pipette in a straight line through the cytoplasm was calculated using the Pythagorean theorem with horizontal (h) and vertical (v) distances:

$$d = \sqrt{h^2 + v^2} \tag{8}$$

In this case, d in Eq. 8 is replaced by $d_{\text{cytoplasm}}$ and h and v correspond to the horizontal and vertical distances, respectively, between the site of sperm attachment and the tip of the patch pipette.

(*b*) The shortest distance (d_{surface}) between the sperm and the tip of the pipette, following a patch over the surface of the egg, was calculated as the sum of two distances: (*a*) the length of an arc between the site of sperm attachment and the site of pipette indentation (see Fig. 1, *X*) on the surface of the egg (the "great circle" route) plus (*b*) the length along the pipette from the site of indentation at the surface of the egg to the tip of the pipette, which pushed the membrane surface deep into the center of the egg.

The length of the arc (arclen) was determined as follows. The length of the chord (d_a) between the site of sperm attachment and the site of pipette indentation was calculated as d in Eq. 8. In this case, h and v correspond to the horizontal and vertical distances, respectively, between the site of sperm attachment and the site of pipette indentation (both at the surface of the egg).

The length of the shortest arc (the distance along the great circle route) over the surface between the sites of sperm attachment and pipette indentation is found using d_a and the diameter of the egg (diameter = 114 μm):

$$\text{arclen} = \left[\pi - \cos^{-1}\left(d_a/\text{diameter}\right)\right] \text{diameter}/2 \tag{9}$$

The distance (piplen) between the site of indentation and the tip of the pipette was determined as d in Eq. 8. In this case, h and v corresponded to the horizontal and vertical distances, respectively, between the site of pipette indentation and the tip of the pipette. The total distance over the surface of the egg (d_{surface}) was then calculated using arclen and piplen:

$$d_{\text{surface}} = \text{arclen} + \text{piplen} \tag{10}$$

Statistics

Results are expressed as mean ± SE for n determinations unless stated otherwise.

RESULTS

Measurements on the voltage clamped plasma membrane of the whole egg and from isolated membrane patches at the surface of the egg using the loose patch clamp

pipette were carried out simultaneously, before and after attachment of a single sperm to the egg (Fig. 1). Immediately after the electrophysiological measurements were completed, the position of the fertilization cone, which served as a marker for the site of sperm attachment and entry, and the location of the tip of the patch pipette were determined. Sperm added to the bath never gained access to the membrane patch. Consequently, the method used cannot record changes at the immediate site of sperm attachment. Other than this restriction, after addition of the sperm to the bath, the site of sperm attachment relative to the location of the membrane patch is random, since for sea urchins the sperm attaches and penetrates the dejellied egg equally well anywhere on the surface (Schroeder, 1980).

Phases of the Activation Current in Whole Eggs

For whole eggs voltage clamped at 0 to −20 mV, every sperm that initiates an electrophysiological response enters the egg and normal development ensues (Lynn and Chambers, 1984; Lynn et al., 1988; Chambers, 1989; McCulloh, 1989).

An activation current of characteristic pattern (Fig. 3 *A*) is initiated within 3 s after attachment of a sperm to the egg (Lynn et al., 1988; Chambers, 1989). The activation current has an abrupt onset, I_{on} (at 0 time), a shoulder or phase 1 during which the inward current slowly increases to a maximum, I_{sm}, followed by the phase of major inward current, phase 2. The latter phase culminates in a peak, I_p. For the experiments reported here, phases 1 and 2 had durations of 11.5 ± 1.5 s (n = 9) and 20 ± 1.0 s (n = 10), respectively. During phase 2, exocytosis of the cortical granules initiates and then propagates as a wave over the surface of the egg (McCulloh, 1984). Phase 3 starts with a rapid cutoff of the inward current following I_p. The duration of phase 3 is arbitrarily defined as the time from its initiation to the time when the current amplitude decreases to a value equal to 10% of I_p (Lynn et al., 1988). In this paper, however, we are only concerned with the changes that occur during phases 1 and 2 and the initial 3–5 s of phase 3. The amplitudes of the currents reflect the conductance changes that occur after attachment of the sperm (see below). The inward currents observed during phases 1 and 2 generate the two positive-going phases of the activation potential observed in eggs that are not voltage clamped (Chambers and de Armendi, 1979; Lynn et al., 1988). It should be noted that the currents associated with the voltage gated action potential mechanism are not involved, since this mechanism is inactivated in eggs voltage clamped at 0 to −20 mV.

Changes in the Patch Clamp Pipette Current and Its Seal Resistance in Relation to the Phases of the Activation Current in the Whole Egg

Simultaneous measurements were made of the whole egg activation current and the current in the patch pipette. An objective of these measurements was to ascertain if currents measured locally with the loose patch clamp were related to voltage clamp currents measured from the whole egg. Currents were measured simultaneously from a whole egg clamped at −20 mV and from the membrane patch by means of the loose patch pipette clamped at nominal 0 mV (close to but not necessarily exactly the same as the bath potential; see Methods). Voltage clamp command steps applied to the patch clamp pipette were superimposed to measure the seal resistance from the amplitude of the resulting pipette current pulses (see Methods).

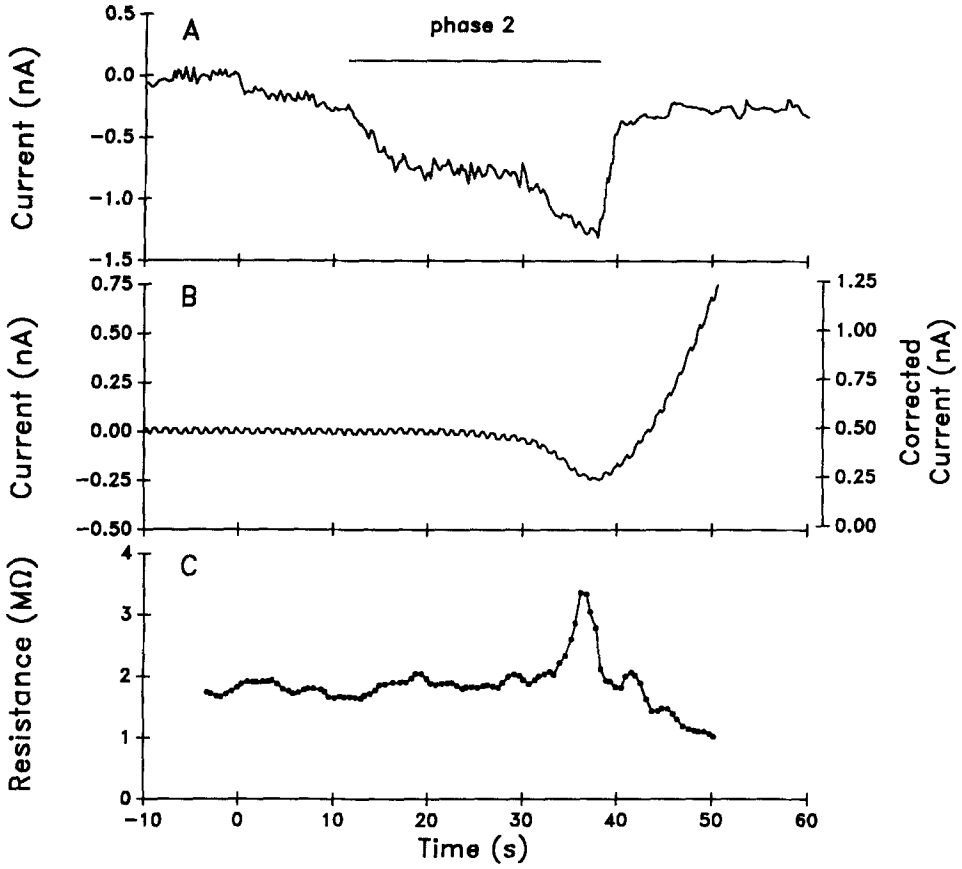

FIGURE 3. Changes of the patch pipette current and patch seal resistance during an egg's activation current initiated by a sperm. (*A*) The activation current monitored by the single microelectrode, switched voltage clamp comprises three phases: phase 1 begins at 0 s, shortly after attachment of a sperm to the surface of the egg, and ends at 11.5 s as phase 2 (labeled horizontal bar) begins; phase 3 begins at the large, rapid decrease of current at 38 s as phase 2 ends. Phase 3 continues beyond the period shown in this figure. Inward current is displayed as a downward deflection of the trace. (*B*) The current flowing through the loose patch clamp pipette measured simultaneously with *A*. Small voltage steps lasting ~0.5 s and repeating roughly every 1 s were superimposed upon the loose patch clamp pipette's holding potential of "nominal" 0 mV. Current pulses through the pipette's seal in response to the voltage steps are seen. Currents flowing out from the pipette (into the egg or the bath) are displayed as downward deflections of the trace. (*C*) The resistance of the seal between the loose patch clamp pipette and the surface of the egg was determined by dividing the amplitude of pipette voltage steps (0.375 mV) by the amplitude of the resulting current steps seen in *B*. Knowledge of both the change of current through the seal (*B*) and the resistance of the seal (*C*) permitted us to estimate the difference of potential between the interior of the pipette and the bath (0.83 mV), assuming all the change of current at the time of the peak seal resistance flowed through the seal resistance. The vertical axis to the right of *B* reflects the current scale corrected by using the calculated offset of the pipette potential.

An example of one of the 52 experiments of this type is shown in Fig. 3. The time course of the whole egg activation current (Fig. 3 *A*), described above, can be compared with the time course of the changes in the observed pipette current (Fig. 3 *B*) and the seal resistance between the pipette and the egg surface (Fig. 3 *C*). A summary of these observations follows:

Patch pipette current. During phase 1 of the activation current, no shift of the current recorded from the patch pipette occurred (0–11.5 s in Fig. 3 *B*). During phase 2, the patch pipette current shifted transiently (downward deflection between 30 and 38 s in Fig. 3 *B*). The transient deflection was downward (out of the pipette) in 14 cases, upward (into the pipette) in 14 cases, and too small to be measured in 3 cases. The peak of the transient shift of the pipette current averaged -0.011 ± 0.0096 nA ($n = 24$) and was not significantly different from 0 ($0.2 < P < 0.4$). The average deviation from this mean (standard deviation or root mean square deviation) was 0.047 nA and serves as a measure of how much the current deviated from 0 nA.

The peak of this transient current occurred during the later half of phase 2 (see further below). The duration of the transient shift (from its onset to the time when the pipette current returned to its initial value) averaged 16.7 ± 0.95 s ($n = 52$).

The transient shift of the pipette current was followed, during the later part of phase 2 or the beginning of phase 3, by a sustained current opposite in direction to the transient shift (after 38 s in Fig. 3 *B*). The amplitude of this shift often was large enough to saturate our recording devices. For those cases where it was small enough to be measured, its standard deviation was 0.16 nA (an underestimate of the average amplitude of the sustained current).

The currents recorded by the patch pipette often exceeded those that we expected to measure from such a small patch of membrane ($< 1\%$ of the egg's plasma membrane) and occasionally exceeded the currents measured simultaneously with the whole egg voltage clamp. Therefore, we suspected that the currents were not flowing through the egg's plasma membrane but rather through the seal resistance between the pipette and the surface of the egg.

Patch pipette seal resistance. The resistance of the seal between the patch pipette and the egg surface (Fig. 3 *C*) was computed (see Methods) from the amplitude of the current pulses superimposed in the trace for the pipette current shown in Fig. 3 *B*. The seal resistance averaged 8 ± 2.0 MΩ ($n = 6$) before insemination of the egg. After insemination, the seal resistance did not change during phase 1 (Fig. 3 *C*). However, during phase 2, the seal resistance transiently increased, attaining a peak of 16 ± 2.8 MΩ ($n = 6$), which was 1.7 ± 0.19-fold ($n = 9$) times the preceding baseline value (Fig. 3 *C*). The peak seal resistance was attained during the later half of phase 2 and coincided with the time for attainment of the peak of the transient shift in pipette current (Fig. 3 *B*). The time course of the increase in seal resistance mirrored the transient shift of current.

After returning to the preceding baseline value, the seal resistance steadily decreased (Fig. 3 *C*) coincidentally with the sustained deflection of pipette current (Fig. 3 *B*), and, in the majority of experiments, could not be measured because the recording device was saturated by the sustained current. In several experiments where the seal resistance could be measured as its sustained value during phase 3, it

averaged 3 ± 1.3 MΩ (n = 3) and was 30 ± 9.5% of the seal resistance before the transient increase.

Origin of the patch pipette current. Even when the interior of the patch pipette was clamped at nominal 0 mV, some pipette current was measured. This can be explained by the inability to eliminate slight potential differences between the virtual grounds maintaining the potentials of the pipette and the bath (see Methods). The relatively large magnitude of the pipette current, averaging ~0.05 nA for the transient peak and >0.16 nA for the sustained current, might result from the changes of seal resistance, which increased to ~170% and then decreased to ~30% of the baseline seal resistance. The difference of potential between the pipette and the bath that would be required to account for the observed pipette currents was calculated from the change of seal resistance and the current offset at the peak of the transient current offset. The average value, −0.3 ± 0.16 mV (n = 4) with a standard deviation of 0.33 mV, is well within the difference of potentials we could have expected using our instrumentation. Therefore, we feel quite certain that the changing seal resistance is sufficient to account for the majority of the pipette current observed using this technique. This explanation is supported by the observation that changes in the amplitude of the pipette current were inversely proportional to the changes in seal resistance; the peak of the transient pipette current correspond in time with the maximum seal resistance and the sustained current (with polarity opposite to that of the transient current) corresponded in time with the sustained, decreased seal resistance. In addition, the observation that roughly one-half of the nonzero pipette currents recorded (14 of 31 responses) were of one polarity, whereas the other half were of the opposite polarity (14 of 31 responses), suggests that the pipette current reverses at a potential very near the bath potential (true 0 mV), a characteristic of currents through leakage pathways.

Changes in Conductance of the Membrane Patch in Relation to Membrane Conductance Changes of the Whole Egg during the Activation Current

In the second series of experiments, the conductances of the whole egg and the membrane patch were measured simultaneously. The objective of these measurements was to ascertain the time when the peak conductance in the egg membrane patch occurred relative to the conductance changes that occur in the whole egg during the activation current. (The relationship between time and distance is discussed in a later section.) Current was recorded from a whole egg clamped at 0 mV, but with superimposed hyperpolarizing voltage clamp command steps −20 mV in amplitude. The conductance of the whole egg was computed during the three phases of the activation current from the amplitude of the resulting whole egg current pulses. Simultaneously, current was recorded from a patch pipette, the interior of which was clamped at nominal 0 mV (see Methods). The conductance in the membrane patch was computed from the amplitude of the current pulses that passed through the patch of the egg membrane in response to the 20-mV hyperpolarizing pulses applied to the whole egg.

An example of one of the 18 experiments of this type is shown in Fig. 4. The time course of the activation current in an egg voltage clamped at 0 mV with superimposed current pulses generated by the 20-mV hyperpolarizing voltage steps (Fig. 4 *A*)

is compared with the time course of the pipette current (Fig. 4 *C*) and the conductance changes in the whole egg (Fig. 4 *B*) and in the patch (Fig. 4 *D*). The three phases of the activation current in the whole egg (described earlier and in Fig. 3 *A*) are shown in Fig. 4 *A*, but with superimposed current pulses. The whole egg

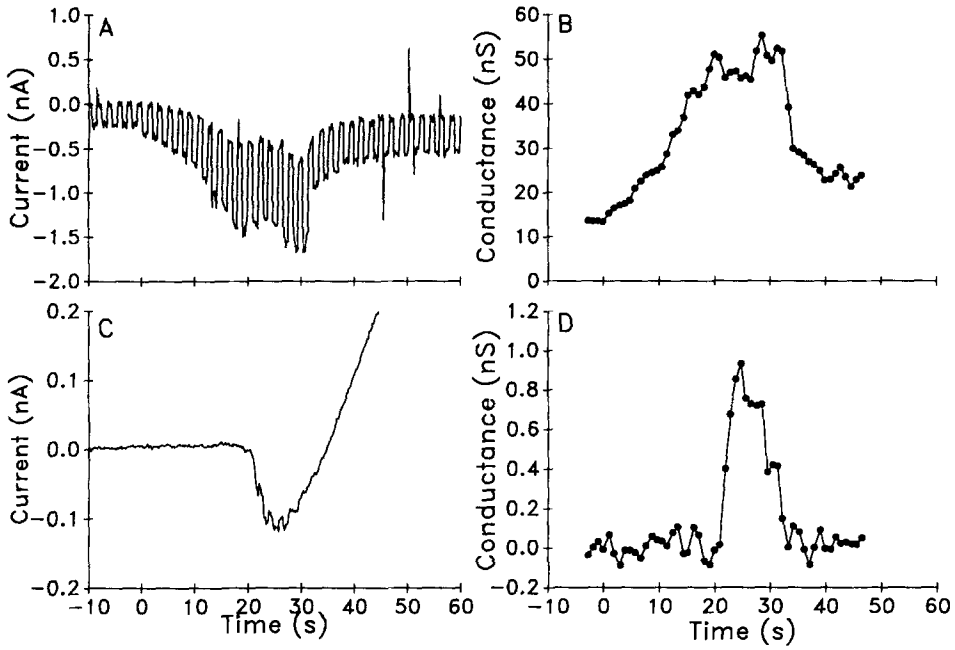

FIGURE 4. Changes of current and membrane conductance for the whole egg and the membrane patch during activation of an egg by a sperm. (*A*) Current flowing through the membrane of the whole egg was recorded using the single microelectrode, switched voltage clamp. The membrane potential was repeatedly stepped between 0 and -20 mV roughly once every 2 s. The current steps in response to these voltage steps are visible in the whole egg membrane current. Inward currents are displayed as downward deflections of the trace. (*B*) The conductance for the membrane of the whole egg was determined by dividing the amplitude of the current pulses in *A* by the amplitude of the voltage steps (20 mV). Phase 1 begins at 0 s. Phase 1 ends and phase 2 begins at 10.5 s. Phase 2 ends and phase 3 begins at 32.5 s. (*C*) The current flowing through the loose patch clamp pipette was recorded simultaneously with the whole egg current. Current pulses in response to steps of the whole egg membrane potential can be seen for only a brief period between 20 and 35 s. Currents flowing out of the pipette (into the egg or the bath) are displayed as downward deflections of the trace. (*D*) The conductance of the membrane patch was determined by dividing the amplitude of the current pulses in *C* by the amplitude of the voltage steps applied to the whole egg's plasma membrane (20 mV).

membrane conductance increased moderately during phase 1 (Fig. 4 *B*), underwent a major increase to attain peak conductance at the time of I_p during phase 2, and then rapidly decreased at the onset of phase 3 (Lynn et al., 1988). The pipette current (Fig. 4 *C*) exhibited both transient and sustained deflections as described above. The

membrane conductance in the patch (Fig. 4 *D*) for every egg examined (n = 18) never increased during the phase 1 increase of conductance observed in the whole egg. This was true irrespective of whether the membrane patch was close to (within 10 μm) or far from the site of sperm attachment. On the other hand, the conductance in the patch (Fig. 4 *D*) always increased, averaging 0.4 ± 0.077 nS (n = 8) for a brief period during the phase 2 major increase in conductance observed in the whole egg. The peak increase of conductance in the patch occurred at different times during phase 2 depending on the distance of the patch from the site of sperm attachment (see further below). In the majority of the experiments, beginning ~5 s after the start of phase 3 of the activation current conductance measurements on the membrane patch could not be continued because the seal resistance decreased below acceptable values. We believe the decrease of seal resistance occurred because of elevation of the fertilization envelope and formation of the hyaline layer at this time.

Characteristics of the conductance increase in the patch during phase 2. Comparison of the conductance increase in the patch with that in the whole egg during phase 2 reveals three important features: (*a*) The duration of the conductance increase in the patch (8.0 ± 0.57 s, n = 10) is significantly shorter than the duration of phase 2 (20 ± 0.99 s, n = 10; $P \ll 0.001$), as can be seen by comparing Fig. 4 *D* with Fig. 4 *B*. (*b*) Although the peak conductance in the patch amounted to 1.6 ± 0.32% (n = 8) of the whole egg conductance, at the corresponding time the surface area of the patch was only 0.55 ± 0.09% (n = 7) that of the whole egg. This percentage of the surface area was calculated from conductance measurements carried out on different eggs before insemination (see Methods). Consequently, the peak conductance in the patch per unit area of membrane was roughly threefold greater than that for the whole egg. (*c*) The peak increase of conductance in the patch occurred at any time during the latter two-thirds of phase 2 in the whole egg, depending on the distance of the patch from the site of sperm attachment, as analyzed more fully below.

Effect of changes in seal resistance on computation of conductance changes in the patch. Changes in the seal resistance affect the amplitude of the membrane currents (and of the current steps used to calculate membrane conductance) measured with the loose patch technique. This is because some of the current flowing through the membrane patch is shunted from the interior of the pipette to the bath through the seal resistance (see Methods, Eq. 7). Therefore, an increase in seal resistance could decrease the shunting of current and thus increase the apparent membrane conductance. However, the increase in seal resistance during phase 2 cannot account for the observed increase in conductance in the membrane patch for the following reasons: (*a*) In the recording configuration used, the resistance of the pipette (R_{pip} = 0.29 ± 0.013 MΩ, n = 14) is a much smaller resistance pathway to ground than the resistance of the seal both before the increase in seal resistance (3.4 ± 0.58 MΩ, n = 14) and at the time of the peak increase in seal resistance (16 ± 2.8 MΩ, n = 6). Substituting the values for R_{pip} and R_s in Eq. 6 shows that 92 and 98% of the current that crossed the egg membrane patch flowed into the pipette before, and at the peak of, the seal resistance increase, respectively. Correspondingly, between 8 and 2% of the current was not measured by the loose patch clamp. Consequently, these calculations show that during the activation current (through the first ~5 s of

phase 3) the seal resistance increase can account for no more than an 8% increase of current in the patch clamp pipette. Currents observed in response to voltage steps applied to the whole egg increased from undetected values before phase 2 to clearly measurable values (as much as a 10-fold increase), clearly more than can be attributed to an increase of the seal resistance. (*b*) Experiments were conducted to ascertain exactly when the peak seal resistance occurred relative to the time of attainment of peak conductance increase in the egg's membrane patch. This was determined by applying voltage steps to the whole egg and the patch pipette alternately, before and during activation of the egg by a sperm. The results showed that although the peak increase in conductance in the membrane patch occurred at the time the seal resistance started to increase, the peak membrane conductance increase still preceded the peak seal resistance by 5 ± 1.4 s (n = 8). Consequently, we conclude that the conductance increase measured with the patch pipette was caused by a change of membrane conductance and could not be explained by changes in the seal resistance. The magnitude of the seal resistance change is too small and the changes of seal resistance do not coincide in time with changes in G_m.

Progression of the Increases in Seal Resistance and Membrane Conductance

Additional objectives of these experiments were to determine whether changes in seal resistance and changes in the conductance for the membrane patch were correlated with the distance of the membrane patch from the site of sperm attachment. Distance was measured in two ways: (*a*) in a straight line ($d_{cytoplasm}$) through the cytoplasm of the egg between the sperm and the tip of the pipette, and (*b*) over the surface of the egg ($d_{surface}$), which includes the arc from the sperm to the site of pipette indentation at the egg's surface plus the distance along the pipette from the site of indentation to the tip of the pipette.

The time of the peak increase in seal resistance is related to the distance between the sperm and the tip of the patch pipette. The peak increase in seal resistance (observed as the peak of the transient deflection of current in the patch pipette) occurred at different times during phase 2. The shortest and longest times after the onset of phase 2 when the peak seal resistance was attained were when the patch was closest and furthest, respectively, from the site of sperm attachment with the distance measured in a straight line through the cytoplasm (Fig. 5 *A*). Within phase 2, the time for the peak increase of seal resistance was well correlated with the distance between the sperm and the tip of the patch pipette (r = 0.72), with distance measured in a straight line through the cytoplasm. The average rate of progression in a straight line through the cytoplasm for the increase of seal resistance was 5.2 ± 0.49 μm/s (n = 8), calculated for each egg as the linear distance divided by the time from onset of phase 2 until the peak of the transient increase of seal resistance occurred. Time is measured from the start of phase 2 of the activation current, since the seal resistance increase generally occurred within phase 2. On the other hand, the time of the peak increase of seal resistance was poorly correlated (r = −0.45) with the distance between the sperm and the tip of the pipette when distance was measured over the surface of the egg (Fig. 5 *B*). Comparison of the sum of the squared deviations for these two models indicates that the data fit significantly better

($0.025 < P < 0.05$; F test) to the model in which distance was measured in a straight line through the cytoplasm.

The time of the peak conductance increase in the patch is related to the distance between the sperm and the tip of the patch pipette. The peak increase of conductance in the patch occurred at different times during phase 2. Within phase 2, the time for the peak

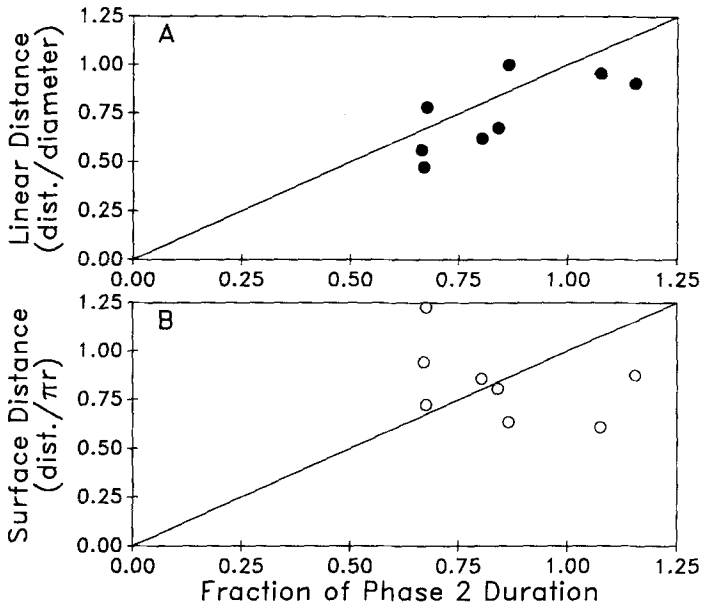

FIGURE 5. Plots comparing the time of occurrence for the peak of the increase of seal resistance with the distance between the membrane patch and the site of sperm attachment. The time of occurrence for the peak of the increase of seal resistance is normalized by dividing the time interval between the onset of phase 2 and the peak of seal resistance by the duration of phase 2. (*A*) The distance between the membrane patch and the site of sperm attachment measured in a straight line through the cytoplasm (*filled circles*) was determined using Eq. 8. Each symbol represents the results obtained from an individual egg. The straight, diagonal line indicates the relationship expected if the message that causes the increase of seal resistance travels at a constant velocity throughout the cytoplasm of the egg during phase 2, starting at the site of sperm attachment. (*B*) The distance between the membrane patch and the site of sperm attachment measured over the surface of the egg (*open circles*) using Eq. 10. The same eight eggs used in *A* are displayed here. The straight, diagonal line indicates the relationship expected if the message that causes the increase of seal resistance travels at a constant velocity along or just beneath the plasma membrane during phase 2, starting at the site of sperm attachment.

conductance of the patch was well correlated ($r = 0.93$) with the distance of the patch from the site of sperm attachment, measuring distance in a straight line through the cytoplasm (Fig. 6 *A*). For each egg, the linear distance between the sperm and the tip of the pipette divided by the time between the onset of phase 2 and the attainment of the peak increase of G_m was calculated as an estimate for the rate of propagation for

this change as it travels through the egg. The average of these estimates was 6.2 ± 0.41 μm/s (n = 10). Time is measured from the start of phase 2 of the activation current, since the patch conductance change occurs only during this period. On the other hand, the time for the peak conductance in the patch was poorly correlated (r = −0.09) with distance measured over the surface of the egg (Fig. 6 *B*). The sum

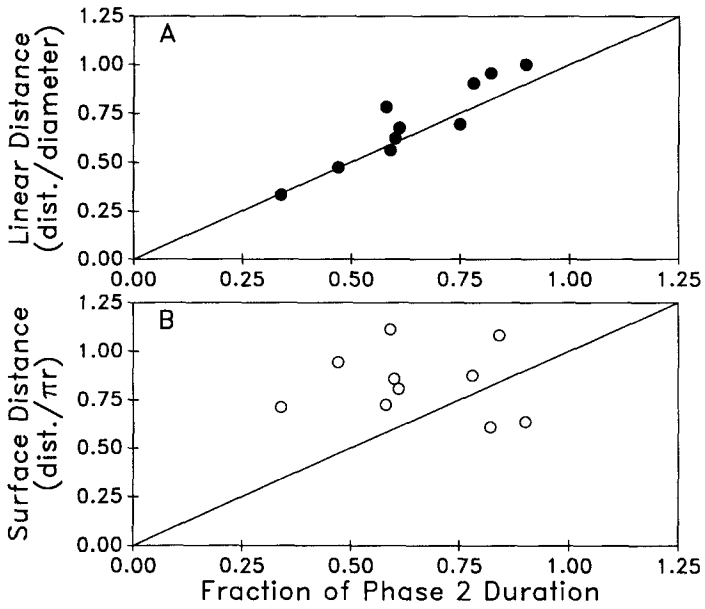

FIGURE 6. Plots comparing the time of occurrence for the peak of conductance of the membrane patch with the distance between the membrane patch and the site of sperm attachment. The time of occurrence for the peak of the increase in patch conductance is normalized by dividing the time interval between the onset of phase 2 and the peak of seal resistance by the duration of phase 2. (*A*) The distance between the membrane patch and the site of sperm attachment measured in a straight line through the cytoplasm (*filled circles*) was determined using Eq. 8. Each symbol represents the results obtained from an individual egg. The straight, diagonal line indicates the relationship expected if the message that causes the increase of membrane conductance travels at a constant velocity throughout the cytoplasm of the egg during phase 2, starting at the site of sperm attachment. (*B*) The distance between the membrane patch and the site of sperm attachment measured over the surface of the egg (*open circles*) using Eq. 10. The same 10 eggs used in *A* are displayed here. The straight, diagonal line indicates the relationship expected if the message that causes the increase of membrane conductance travels at a constant velocity along or just beneath the plasma membrane during phase 2, starting at the site of sperm attachment.

of the squared deviations between the data and the two different models were significantly different (P < 0.01) and the data fit better to the model in which distance was measured in a straight line through the cytoplasm.

Comparison of the rates of progression for the changes of seal resistance and membrane conductance and for the exocytosis of cortical granules. The rates of progression amounted

to 5.2 ± 0.49 μm/s (n = 8) and 6.2 ± 0.41 μm/s (n = 10) for the peak increase in seal resistance and the peak increase of conductance, respectively. These values can be converted to transit times by dividing the diameter of the egg (114 μm; McCulloh et al., 1987) by the rate of progression. Transit times are 22 ± 2.1 s (n = 8) and 18 ± 1.1 s (n = 10) for the increase of seal resistance and membrane conductance, respectively. The transit time for the progression of exocytosis across the egg was determined by measuring the interval between the time when the fertilization envelope starts to elevate at the site of sperm attachment and the time when elevation begins at the antipode. Although the cortical change (exocytosis) shortly procedes elevation of the fertilization envelope, the progress of elevation of the envelope faithfully reproduces the rate at which exocytosis progresses around the egg (Moser, 1939; Kacser, 1955). The transit time for the occurrence of exocytosis averages 23 ± 4.3 s (n = 5), equivalent to a rate of progression across the egg (diameter of the egg divided by the transit time) of 5.5 ± 0.72 μm/s (n = 5). This rate is indistinguishable from the rate of progression across the egg of each of the two impedance changes since these three rates (and transit times) are not significantly different ($P > 0.05$; ANOVA).

Despite their similar rates of progression, the increases of conductance and seal resistance do not occur exactly at the same time. The maximal increase of conductance for the membrane patch was attained 5 ± 1.4 s (n = 8) before the attainment of the maximum of the transient increase of seal resistance (monitored as the transient pipette current). The cortical granule exocytosis occurs during the same period of time (phase 2; McCulloh, 1984), although simultaneous recordings of all three events have not been made.

DISCUSSION

The loose patch clamp method was applied to ascertain whether the conductance changes that generate the three phases of the activation current, observed in whole eggs following a successful attachment of the sperm, are global or localized. No conductance changes could be detected in the patch during phase 1. However, during phase 2, the phase of major conductance increase in the whole egg, a transient increase of conductance in the patch of much shorter duration was observed in every patch examined, the time of occurrence depending on the linear distance (through the egg) of the patch from the site of sperm attachment. An additional finding was that the resistance of the seal between the patch pipette and the egg surface also did not change during phase 1, but underwent a transient increase in resistance during phase 2. The time when the transient increase in seal resistance occurred during phase 2 also depended on the distance of the patch from the site of sperm attachment. After the onset of phase 3 the seal resistance rapidly decreased. Knowledge of the changes of seal resistance was necessary before performing the conductance measurements and important for validation of the membrane conductance changes.

Membrane Conductance of the Patch Does Not Change during Phase 1

An increase in membrane conductance of the patch during phase 1 of the activation current could not be detected in any of the experiments carried out. Clearly the

sperm cannot gain access to the patch circumscribed by the orifice of the pipette. This suggests that the conductance increase measured by the whole egg voltage clamp during phase 1 (Fig. 4 *B*) is localized to a region at, or in the immediate vicinity of, the site of sperm attachment, since this is a region that cannot be directly sampled by the patch pipette. Alternatively, the conductance changes could be uniformly distributed over the entire surface of the egg and the local conductance increase would then be difficult to detect. However, we have recently obtained conclusive evidence, in experiments where the sperm was introduced into the lumen of the loose patch clamp pipette, that the conductance increase during phase 1 is indeed localized to the site of sperm attachment in sea urchin eggs (McCulloh and Chambers, 1986*b*). In addition, our finding that when more than one sperm attaches to the egg during phase 1, the currents elicited by each sperm sum (Lynn et al., 1988) indicates that each sperm opens only a fraction of the available channels, suggesting that the channels that opened were in the neighborhood of the attached sperm, rather than globally distributed. These results are similar to those reported for the egg of the echiuroid worm, *Urechis*, for which evidence has been presented that the fertilizing sperm opens channels limited to, or in the immediate vicinity of, the site of sperm entry (Jaffe et al., 1979; Gould-Somero, 1981). Unlike the sea urchin egg, however, in *Urechis* eggs a second phase of channel openings, associated with an exocytotic response, does not occur.

An explanation for the absence during phase 1 of a change in the resistance of the seal between the patch pipette and the egg surface is that exocytosis of the cortical granules and elevation of the fertilization envelope do not occur during this period.

Evidently, during phase 1, equal in duration to the latent period (Allen and Griffin, 1958), time-consuming processes take place in preparation for the phase 2 conductance changes. This includes activation of the phosphoinostide cycle and generation of inositol trisphosphate (Turner et al., 1984; Kamel et al., 1985), processes that may subsequently initiate (during phase 2) the wave of increased free Ca^{2+} (Whitaker and Irvine, 1984; Swann and Whitaker, 1986).

A Transient Increase in Membrane Conductance Progresses over the Surface of the Egg during Phase 2

Clearly the increase in conductance observed during phase 2 of the activation current in the whole egg does not occur uniformly over the surface of the egg. Our data on the magnitude per unit area, duration, and timing of the conductance increase in the patch indicate that the major conductance increase during phase 2 for the whole egg represents the net result of a brief turning on, lasting ~8 s and then turning off, of membrane conductance in a localized zone of the egg membrane that progresses, with a transit time of ~18 s over the entire egg surface. Evidently, during phase 2 an increase in membrane conductance starts at the site of sperm attachment and sweeps as an encircling band over the surface of the egg to the opposite pole, while behind the advancing band the conductance increase turns off. The explanation for the fact that the transit time for the peak increase in conductance (~18 s) determined from patch clamp measurements is not significantly different from the duration of phase 2 (~20 s; see Table I) of the activation current in the whole egg is because the conductance increase during phase 2 (see Fig. 4 *B*) lasts only as long as the encircling

band of conductance increase moves across the egg. The rapid cutoff of conductance in the whole egg after phase 2 (Fig. 4 *B*; also see Lynn et al., 1988) reflects the turn off of conductance at the trailing edge of the encircling band as it invades the antipode of the egg, reducing the current to a level close to that attained at the end of phase 1.

The findings presented here for the phase 2 conductance increase resemble those observed during fertilization of the amphibian egg (Schlichter, 1989). Using either a vibrating probe or a patch electrode, a transient inward current localized to a ring-shaped zone was found to progress over the entire egg surface as a wave starting from the point of activation (Jaffe et al., 1985; Kline and Nuccitelli, 1985; Kline, 1986). This wave, the same as we find for the sea urchin egg, shortly preceded the wave of exocytosis.

TABLE I

Transit Times in Sea Urchin Eggs

Parameter investigated	Transit time (mean ± SE)
Lytechinus variegatus (this paper)*	*s*
Peak increase in seal resistance	18 ± 1.1 (10)
Peak increase in membrane conductance	22 ± 2.1 (8)
Elevation of fertilization envelope	23 ± 4.3 (5)
Duration of phase 2	20 ± 1.0 (10)
Lytechinus pictus‡	
Elevation of fertilization envelope§ (exocytosis)	24 ± 1.5 (15)
Elevation of intracellular $[Ca^{2+}]$‖	~25

*Egg diameter 114 ± 1.2 μm (n = 20), T = 22–23°C.
‡Egg diameter 114 μm, T = 16°C.
§Whitaker and Irvine (1984).
‖Swann and Whitaker (1986).

A Transient Increase in Resistance of the Seal between the Patch Pipette and Egg Surface Also Progresses over the Egg during Phase 2

The most obvious currents measured using the loose patch clamp were attributed to the changes in R_s. The currents measured can be explained as flow of current between the interior of the pipette and the bath each maintained at a slightly different potential (~0.33 mV) despite our best attempts to maintain them at exactly the same potential.

Like the membrane conductance increase in the patch, the transient increase in the resistance of the seal between the patch pipette and egg surface starts at the site of sperm attachment and progresses over the surface of the egg to the antipode during phase 2. The membrane conductance increase of the patch that progresses at the same velocity, however, precedes the transient increase in seal resistance by ~5 s. A possible cause of the increase in seal resistance is that this is a consequence of the increase in surface area, which accompanies exocytosis of cortical granules and may result in a greater area of close contact between the rim of the pipette orifice and the plasma membrane of the egg. The transiency of the increase in resistance of the seal

between the patch pipette and egg surface, followed by a marked, rapid decrease of the seal resistance probably reflects separation of the pipette tip from the surface of the egg due to elevation and hardening of the fertilization envelope, as well as accumulation of the calcium insoluble hyaline layer material, a product of the exocytosed cortical granules (Chambers and Chambers, 1961). Alternate explanations might involve the wave of cortical contraction seen in these eggs (McCulloh and Chambers, 1987).

A Message Progresses through the Cytoplasm

The progression across the egg at the same velocity (Table I) and at roughly the same time for the transient increase in membrane conductance, the transient increase in seal resistance between the patch pipette and egg surface, and the elevation of the fertilization envelope is consistent with the conclusion that these events are triggered by a common message which originates in the egg at the site of sperm attachment and then progresses to the opposite pole of the egg. It is unlikely that two or three independent mechanisms for signaling would occur nearly simultaneously and have such similar rates of progression, although this possibility cannot formally be excluded at this time.

The peak seal resistance increase occurs several seconds after the peak increase in conductance. If these two events share a common trigger, they must have two different thresholds or else a physiological delay must exist involving more or slower steps for the changes of seal resistance after triggering by a common message. To determine when the elevation of the fertilization envelope occurs relative to the other two events, simultaneous measurements of G_m, R_s, and elevation of the fertilization envelope are required. This was not possible because the pipette indenting the surface of the egg obscured from view the elevation of the fertilization envelope at the membrane patch both by minimizing the thickness of the perivitelline space in the region of contact and by optical distortion. The near simultaneity for these different impedances could result if the ion channels reponsible for the transient increase of G_m are located in the membrane of cortical granules. Conductance increases would appear only after the membrane fusion of cortical granules with the plasma membrane. Alternatively, the opening of channels may precede exocytosis, providing a localized band of sodium influx which could play a role in exocytosis.

The data presented in this paper indicate that the common message progresses through the cytoplasm of the egg (Fig. 1), rather than only through the cortical region. This conclusion is supported by the strong correlation between the linear distance (measured through the cytoplasm) from the site of sperm attachment to the patch, and both the times of occurrence of peak increase in membrane conductance of the patch and of the peak increase in seal resistance (Figs. 5 and 6). That the message progresses through the cytoplasm rather than being restricted to the cortical region can be shown qualitatively by reference to Fig. 1 *A*. Because the patch clamp pipette indents the egg surface (including the cortical region), a sperm at site *a* is far closer to the patch than is, for example, a sperm located at site *b*, provided distances are measured in a straight line through the cytoplasm. Our observations show that the conductance increase occurs earliest when the sperm attaches in close proximity to the patch (see Fig. 6 *A*), as is the case for a sperm located at site *a* (Fig. 1 *A*). If

progression of the message were restricted to the cortical region of the egg, then, contrary to what is observed, a sperm at site *b* should have initiated a conductance increase in the patch well before a sperm at site *a*, since the distance around the cortex of the egg (including the part indented by the pipette) to the patch is much greater in the case of a sperm at site *a*.

It is not clear how deep into the substance of the egg a message generated in the cortical region must reach to appear not to be restricted to the cortical regions using the experimental paradigm and statistical comparison that we have used. No known barriers to diffusion exist in the egg that could restrict diffusion of a small molecule to the cortical region. Restriction of the progression of message to the cortical regions would require that progression involve chemical reactions and that one or more of the metabolites be restricted to the cortex. Only under such conditions would progression be more rapid through the cortical regions than through the center of the egg. The poor correlations of time with distance measured over the surface of the egg certainly provide no evidence for propagation restricted to the cortical region.

The nature of the message is unknown. A change of membrane potential can be ruled out, since in our experiments the membrane potential was held constant by voltage clamp. A likely candidate is an elevation of cytoplasmic free calcium. Evidence that the phase 2 conductance increase in the sea urchin egg is due to a calcium-activated conductance is suggested by the stimulation of a response resembling phase 2 of the activation potential, associated with the occurrence of exocytosis, after the application of the calcium ionophore A23187 to introduce calcium ions into the cytoplasm (Chambers et al., 1974). In addition, microinjection of the calcium chelating agent, EGTA, eliminates the phase 2 increase in conductance (Swann, K., D.H. McCulloh, E.L. Chambers, and M.J. Whitaker, unpublished observations). The phase 2 conductance increase in the sea urchin egg is largely due to the opening of sodium channels (Lynn and Chambers, 1983). A calcium-activated conductance has been shown to contribute to generation of the activation (or fertilization) potential in eggs of other species (Kozuka and Takahashi, 1982; Jaffe et al., 1985; Kline et al., 1986; Schlichter, 1989).

An increase of intracellular free calcium is clearly associated with the occurrence of exocytosis in eggs of the sea urchin and other species (Jaffe, 1985; Whitaker and Steinhardt, 1985; Swann and Whitaker, 1986; Yoshimoto et al., 1986). Like the message that initiates the increase in conductance and the exocytotic response, the increased concentration of free intracellular calcium spreads across the egg (Steinhardt et al., 1977; Poenie et al., 1985) starting from the point of sperm attachment (Eisen et al., 1984; Swann and Whitaker, 1986; Hafner et al., 1988) at a time that approximates the onset of phase 2 of the activation current (Eisen et al., 1984; Whitaker et al., 1989). That the calcium wave travels as a sharp zone across the sea urchin egg (Hafner et al., 1988) is consistent with the concept that the elevated free calcium is the message responsible for the increase of conductance in a localized zone of the egg membrane, which we infer from our measurements sweeps across the egg during phase 2. Moreover, measurements in sea urchin eggs of the time required for the wave of increased free calcium to spread across the egg (Eisen et al., 1984; Swann and Whitaker, 1986; Yoshimoto et al., 1986; Hafner et al., 1988) are in the same range that we have found for the transit times for the peak increase in patch

conductance, seal resistance, and exocytosis (Table I). A precise temporal comparison, however, cannot be made because the calcium measurements were carried out on eggs of sea urchin species, and at temperatures different from those we used.

The release of intracellular stores of calcium is not restricted to cortical regions of sea urchin eggs (Eisen and Reynolds, 1985). They found that the release of calcium is localized principally to the stratified hyaline or cytoplasmic zone of the sea urchin egg (*Arbacia*) stratified by centrifugation. If the calcium wave were restricted only to the cortical region, an aequorin signal indicative of calcium release would have been observed over the entire egg, since the cortical gel (in which the cortical granules are embedded) is not displayed by centrifugation (Moser, 1939; Harvey, 1946). In the hamster egg the transient increases in intracellular concentration of free calcium observed after sperm attachment occur to the same level both in the cortical region and deep in the cytoplasm (Igusa and Miyazaki, 1986). For the amphibian egg, a wave of increased free calcium that spreads through the subcortical cytoplasm (Busa and Nuccitelli, 1985) from the site of sperm–egg interaction has been implicated in the progression of a wave of increased conductance over the egg surface (Jaffe et al., 1985; Schlichter, 1989).

It is clear that the message that causes the increases in G_m and R_s progresses throughout the egg, although our data do not indicate whether the progression occurs by diffusion or by propagation of an autocatalytic wave. The elevation of calcium throughout the egg is believed to be caused by propagation of an autocatalytic wave. One such autocatalytic scheme (Ehrenstein and Fitzhugh, 1986) involves elevation of intracellular calcium, which stimulates the production of inositol trisphosphate (Whitaker and Irvine, 1984), and inositol trisphosphate in turn leads to release of calcium from intracellular stores (Turner et al., 1984; Swann and Whitaker, 1986), thus completing a positive feedback cycle. An autocatalytic wave would be likely to result in a constant velocity of progression throughout the cytoplasm of the egg.

CONCLUSION

Analysis of the early events of sperm–egg interaction led Sugiyama (e.g., 1953, 1956) and Yamamoto (reviewed in Yamamoto, 1961) to conclude that an invisible fertilization wave or impulse underlies the propagation around the egg of the exocytotic process in the sea urchin and the fish, respectively. Our data indicate that a wave of excitation travels from the site of sperm attachment throughout the substance of the egg. Progression of an activating wave through the entire cytoplasm of the egg, rather than only at or near the surface, may serve an important role in synchronizing activation throughout the egg of both surface events such as the increase of membrane conductance and the exocytosis of cortical granules, as well as deep cytoplasmic events such as metabolic derepression, protein synthesis, and onset of development.

The authors wish to thank Dr. David Landowne for critical review of an early version of this manuscript. We also wish to thank Dr. David Weiss for comments on some of the particularly pedantic prose in one portion of the procedures. We thank Dr. Wolfgang Nonner for help with the design of the loose patch clamp. We thank Helene Hanchett for drawing Fig. 1.

This research was supported by NIH fellowship award HD-06505 to D.H. McCulloh, by NIH research grant HD-19126 to E.L. Chambers, and by NSF research grants PCM 83-16864 and DCB 87-11787 to E.L. Chambers.

Original version received 25 May 1990 and accepted version received 1 October 1990.

REFERENCES

Allen, R. D., and J. L. Griffin 1958. The time sequence of early events in the fertilization of sea urchin eggs. I. The latent period and the cortical reaction. *Experimental Cell Research.* 15:163–173.

Busa, W. B., and R. Nuccitelli. 1985. An elevated free cytosolic Ca^{2+} wave follows fertilization in eggs of the frog, *Xenopus laevis*. *Journal of Cell Biology.* 100:1325–1329.

Chambers, E. L. 1989. Fertilization in voltage-clamped sea urchin eggs. *In* Mechanisms of Egg Activation. R. Nuccitelli, G. N. Cherr, and W. H. Clark, Jr., editors. Plenum Publishing Corp., New York. 1–18.

Chambers, R., and E. L. Chambers. 1961. Explorations into the Nature of the Living Cell. Harvard University Press, Boston, MA. 352 pp.

Chambers, E. L., and J. de Armendi. 1979. Membrane potential of eggs of the sea urchin, *Lytechinus variegatus*. *Experimental Cell Research.* 122:203–218.

Chambers, E. L., B. C. Pressman, and B. Rose. 1974. The activation of sea urchin eggs by the divalent ionophores A 23187 and X-537 A. *Biochemical and Biophysical Research Communications.* 60:126–132.

Ehrenstein, G., and R. Fitzhugh. 1986. A channel model for development of the fertilization membrane in sea urchin eggs. *In* Ionic Channels in Cells and Model Systems. R. Latorre, editor. Plenum Publishing Corp., New York. 421–430.

Eisen, A. D., D. Kiehart, J. Wieland, and G. T. Reynolds. 1984. Temporal sequence and spatial distribution of early events of fertilization in single sea urchin eggs. *Journal of Cell Biology.* 99:1647–1654.

Eisen, A. D., and G. T. Reynolds. 1985. Sources and sinks for the calcium released during fertilization of single sea urchin eggs. *Journal of Cell Biology.* 100:1522–1527.

Epel, D., A. M. Weaver, and D. Mazia. 1970. Methods for removal of the vitelline membrane of sea urchin eggs. *Experimental Cell Research.* 61:64–68.

Fishman, H. M. 1975. Patch voltage clamp of squid axon membrane. *Journal of Membrane Biology.* 24:265–277.

Gould-Somero, M. 1981. Localized gating of egg Na^+ channels. *Nature.* 291:254–256.

Hafner, M., C. Petzelt, R. Nobiling, J. B. Pawley, D. Kramp, and G. Schatten. 1988. Wave of free calcium at fertilization in the sea urchin egg visualized with Fura-2. *Cell Motility and the Cytoskeleton.* 9:271–277.

Harvey, E. B. 1946. Structure and development of the clear quarter of the *Arbacia punctulata* egg. *Journal of Experimental Zoology.* 102:253–276.

Igusa, Y., and S. Miyazaki. 1986. Periodic increase of cytoplasmic calcium in fertilized hamster eggs measured with calcium-sensitive electrodes. *Journal of Physiology.* 377:193–205.

Jaffe, L. A. 1976. Fast block to polyspermy in sea urchin eggs is electrically mediated. *Nature.* 261:68–71.

Jaffe, L. A., M. Gould-Somero, and L. Holland. 1979. Ionic mechanism of the fertilization potential of the marine worm, *Urechis caupo*. *Journal of General Physiology.* 73:469–492.

Jaffe, L. A., R. T. Kado, and L. Muncy. 1985. Propagating potassium and chloride conductances during activation and fertilization of the egg of the frog *Rana pipiens*. *Journal of Physiology.* 368:227–242.

Jaffe, L. F. 1985. The role of calcium explosions, waves, and pulses in activating eggs. *In* Biology of Fertilization. Vol. 3. C. B. Metz and A. Monroy, editors. Academic Press, Inc., New York. 127–165.

Kacser, H. 1955. The cortical changes on fertilization of the sea-urchin egg. *Journal of Experimental Biology.* 32:451–467.

Kamel, L. C., J. Bailey, L. Schoenbaum, and W. Kinsey. 1985. Phosphotidylinositol metabolism during fertilization in the sea urchin egg. *Lipids.* 20:350–356.

Kline, D. 1986. A direct comparison of the extracellular currents observed in the activating frog egg with the vibrating probe and patch clamp techniques. *In* Development. R. Nuccitelli, editor. Alan R. Liss, Inc., New York. 1–8.

Kline, D., L. A. Jaffe, and R. T. Kado. 1986. A calcium activated sodium conductance contributes to the fertilization potential in the egg of the Nemertean worm, *Cerebratulus lacteus. Developmental Biology.* 117:184–193.

Kline, D., and R. Nuccitelli. 1985. The wave of activation current in the *Xenopus* egg. *Developmental Biology.* 111:471–487.

Kozuka, M., and K. Takahashi. 1982. Changes in holding and ion-channel current during activation of an ascidian egg under voltage clamp. *Journal of Physiology.* 323:267–286.

Lynn, J. W., and E. L. Chambers. 1983. Ion substitution studies on inseminated voltage clamped eggs of the sea urchin, *Lytechinus variegatus. Journal of Cell Biology.* 97:25*a*. (Abstr.)

Lynn, J. W., and E. L. Chambers. 1984. Voltage clamp studies of fertilization in sea urchin eggs. I. Effect of clamped membrane potential on sperm entry, activation, and development. *Developmental Biology.* 102:98–109.

Lynn, J. W., D. H. McCulloh, and E. L. Chambers. 1988. Voltage clamp studies of fertilization in sea urchin eggs. II. Current patterns in relation to sperm entry, non-entry, and activation. *Developmental Biology.* 128:305–323.

McCulloh, D. H. 1984. Cortical reaction of sea urchin eggs: rate of propagation and extent of exocytosis revealed by membrane capacitance. *Development, Growth and Differentiation.* 27:178. (Abstr.)

McCulloh, D. H. 1989. Sperm entry in sea urchin eggs: recent inferences concerning its mechanism. *In* Mechanisms of Egg Activation. R. Nuccitelli, G. N. Cherr, and W. H. Clark, Jr., editors. Plenum Publishing Corp., New York. 19–42.

McCulloh, D. H., and E. L. Chambers. 1985. Localization and propagation of membrane conductance changes during fertilization in eggs of the sea urchin *Lytechinus variegatus. Journal of Cell Biology.* 101:230*a*. (Abstr.)

McCulloh, D. H., and E. L. Chambers. 1986*a*. Changes of loose patch clamp seal resistance associated with exocytosis of cortical granules in relation to changes of patch membrane conductance in eggs of the sea urchin *Lytechinus variegatus. Biophysical Journal.* 49:178*a*. (Abstr.)

McCulloh, D. H., and E. L. Chambers. 1986*b*. When does the sperm fuse with the egg? *Journal of General Physiology.* 88:38*a*–39*a*. (Abstr.)

McCulloh, D. H., and E. L. Chambers. 1987. Where does the activation wave of the sea urchin egg propagate? *Journal of Cell Biology.* 105:239*a*. (Abstr.)

McCulloh, D. H., J. W. Lynn, and E. L. Chambers. 1987. Membrane depolarization facilitates sperm entry, large fertilization cone formation and prolonged current responses in sea urchin oocytes. *Developmental Biology.* 124:177–190.

Moser, F. 1939. Studies on a cortical layer response to stimulating agents in the *Arbacia* egg. I. Response to insemination. *Journal of Experimental Zoology.* 80:423–445.

Neher, E., and H. D. Lux. 1969. Voltage clamp of *Helix pomatia* neuronal membrane: current measurement over a limited area of the soma membrane. *Pflügers Archiv.* 311:272–277.

Poenie, M., J. Alderton, and R. Y. Tsien. 1985. Changes of free calcium levels with stages of the cell division cycle. *Nature.* 315:147–149.

Schlichter, L. C. 1989. Ion channels in *Rana pipiens* oocytes: changes during maturation and fertilization. *In* Mechanisms of Egg Activation. R. Nuccitelli, G. N. Cherr, and W. H. Clark, Jr., editors. Plenum Publishing Corp., New York. 89–132.

Schroeder, T. E. 1980. Expressions of the prefertilization polar axis in sea urchin eggs. *Developmental Biology.* 79:428–443.

Steinhardt, R. A., L. Lundin, and D. Mazia. 1971. Bioelectric responses of the echinoderm egg to fertilization. *Proceedings of the National Academy of Sciences, USA.* 68:2426–2430.

Steinhardt, R. A., R. S. Zucker, and G. Schatten. 1977. Intracellular calcium release at fertilization in the sea urchin egg. *Developmental Biology.* 58:185–196.

Stühmer, W., W. H. Roberts, and W. Almers. 1983. The loose patch clamp. *In* Single Channel Recording. B. Sakmann and E. Neher, editors. Plenum Publishing Corp., New York. 123–132.

Sugiyama, M. 1953. Physiological analysis of the cortical response of the sea urchin egg to stimulating agents. I. The propagating or non-propagating nature of the cortical changes induced by various reagents. *Biological Bulletin.* 104:216–223.

Sugiyama, M. 1956. Physiological analysis of the cortical response of the sea urchin egg. *Experimental Cell Research.* 10:364–376.

Swann, K., and M. J. Whitaker. 1986. The part played by inositol trisphosphate and calcium in the propagation of the fertilization wave in sea urchin eggs. *Journal of Cell Biology.* 103:2333–2342.

Turner, P. R., M. P. Sheetz, and L. A. Jaffe. 1984. Fertilization increases the polyphosphoinositide content of sea urchin eggs. *Nature.* 310:414–415.

Whitaker, M. J., and R. F. Irvine. 1984. Microinjection of inositol trisphosphate activates sea urchin eggs. *Nature.* 312:636–638.

Whitaker, M. J. and R. A. Steinhardt. 1983. Evidence in support of the hypothesis of an electrically mediated fast block to polyspermy in sea urchin eggs. *Developmental Biology.* 95:244–248.

Whitaker, M. J., and R. A. Steinhardt. 1985. Ionic signaling in the sea urchin egg at fertilization. *In* Biology of Fertilization. Vol. 3. C. B. Metz and A. Monroy, editors. Academic Press, Inc., New York. 167–221.

Whitaker, M. J., K. Swann, and I. Crossley. 1989. What happens during the latent period at fertilization. *In* Mechanisms of Egg Activation. R. Nuccitelli, G. N. Cherr, and W. H. Clark, Jr., editors. Plenum Publishing Corp., New York. 157–171.

Wilson, W. A., and M. M. Goldner. 1975. Voltage clamping with a single microelectrode. *Journal of Neurobiology.* 6:411–422.

Yamamoto, T. 1961. Physiology of fertilization in fish eggs. *International Reviews of Cytology.* 12:361–405.

Yoshimoto, Y., T. Iwamatsu, K. Kirano, and Y. Hiramoto. 1986. The wave pattern of free calcium release upon fertilization in Medaka and sand dollar eggs. *Development, Growth and Differentiation.* 28:583–596.